



HAL
open science

New hybrid polyoxometalate/polymer composites for photodegradation of eosin dye

Mariem Ghali, Chaima Brahmi, Mahmoud Bentifa, Frederic Dumur, Sylvain Duval, Corine Simonnet-Jegat, Fabrice Morlet-Savary, Salah Jellali, Latifa Bouselmi, Jacques Lalevee

► **To cite this version:**

Mariem Ghali, Chaima Brahmi, Mahmoud Bentifa, Frederic Dumur, Sylvain Duval, et al.. New hybrid polyoxometalate/polymer composites for photodegradation of eosin dye. *Journal of Polymer Science Part a-Polymer Chemistry*, 2019, 57 (14), pp.1538–1549. 10.1002/pola.29416 . hal-02491498

HAL Id: hal-02491498

<https://hal.science/hal-02491498>

Submitted on 8 Jul 2020

HAL is a multi-disciplinary open access archive for the deposit and dissemination of scientific research documents, whether they are published or not. The documents may come from teaching and research institutions in France or abroad, or from public or private research centers.

L'archive ouverte pluridisciplinaire **HAL**, est destinée au dépôt et à la diffusion de documents scientifiques de niveau recherche, publiés ou non, émanant des établissements d'enseignement et de recherche français ou étrangers, des laboratoires publics ou privés.

New hybrid polyoxometalate/polymer composites for photodegradation of eosin dye

Mariem Ghali^{a,b,c,d}, Chaima Brahmi^{a,b,c,d}, Mahmoud Benlifa^{*b}, Frédéric Dumur,^e Sylvain Duval,^f Corine Simonnet-Jégat,^g Fabrice Morlet Savary^{a,b}, Salah Jellali^c, Latifa Bousselmi^c, Jacques Lalevée^{*a,b}

^a University of Haute-Alsace, CNRS, IS2M UMR 7361, F-68100 Mulhouse, France

^b University de Strasbourg, France

^c Wastewaters and Environment Laboratory, Center for Water Research and Technologies CERTE, BP 273, Soliman 8020, Tunisia

^d University of Carthage, National Institute of Applied Sciences and Technology, North urban center, Tunis 1080, Tunisia

^e Aix Marseille Univ, CNRS, ICR, UMR7273, F-13397 Marseille (France)

^f Unité de Catalyse et Chimie du Solide (UCCS) – UMR CNRS 8181, Université de Lille Nord de France, USTL-ENSCL, Bat C7, BP 90108, 59652 Villeneuve d'Ascq, France

^g Institut Lavoisier de Versailles, UMR CNRS 8180, Université Paris Saclay, Université de Versailles St-Quentin en Yvelines, 45 Avenue des Etats-Unis, 78035 Versailles cedex (France)

*Corresponding author: Jacques.lalevee@uha.fr

Abstract

New polyoxometalate/polymer hybrid POM composites were prepared by photopolymerization under mild conditions for processable photocatalytic processes. Polyoxometalates Keggin type were incorporated with special photosensitive resin to be photopolymerized under visible light and to obtain new material with photocatalytic activity for dye removal. The synthesized composites were characterized by real-time FT-IR and the photocatalytic ability was investigated on Eosin-Y removal using photolysis under near UV irradiation. Interestingly, the polyoxometalates keep their photocatalytic properties while incorporated into the polymeric matrix since very high conversion rates of Eosin-Y were achieved. Indeed, degradation efficiencies of about 98% and 93% were registered when using $\text{H}_3\text{PMo}_{12}\text{O}_{40}$ /polymer and 94% for $\text{SiMo}_{12}\text{O}_{40}(\text{IPh}_2)_4$ /polymer composites, respectively.

These first results reported in this paper show that the new synthesized composites POM/polymer could be considered as promising materials for the green removal of organic dyes from aqueous solutions.

1. Introduction

With the industrial revolution, the demand in organic dyes for coloring industrial items is massive leading to nearly 10.000 types of dyes and pigments.¹ Most of them are toxic and could be released at relatively high concentrations during the industrial processes.² As a consequence, their removal from industrial effluents is indispensable and considered as a main environmental challenge since they are difficult to biodegrade and tribute undesirable color to water.³ Various physical, chemical and biological methods have been investigated for dyes removal from liquid effluent including the use of Advanced Oxidation Process (AOP).⁴ Photocatalytic degradation is one of the AOP techniques where many metal oxides such as TiO₂, ZnO and WO₃ were tested.⁵ They have been studied for heterogeneous photocatalysis⁶ and employed also with additives such as H₂O₂ and persulfate (S₂O₈²⁻) to improve the quantum yield of organic dye decolorization and degradation under sunlight.⁵ However, polyoxometalates (POMs), which the history goes back to 19th century, have been recently pointed out as an innovative research topic especially when used in the photocatalytic fields.⁷ Actually, POMs are a class of transition metal-oxide clusters mainly of tungsten and molybdenum.⁸ More precisely, they are composed of metal ions in their highest oxidation state bridged by oxo ligands, and any other element can be linked to the POM framework which leads to versatile structures and therefore different properties.^{9,10} Besides their low toxicity and cost, POMs has various interesting properties including Bronsted acidity, redox properties, oxidative and thermal stability and especially strong absorption of UV light.¹¹

Indeed, POMs become powerful oxidizing compounds upon the UV illumination ($\lambda < 400\text{nm}$) where their excited states can undergo fast and reversible electrons transfer without structural changes.¹² Therefore, POMs have been exploited to solve many environmental issues such as the sequestration of toxic gases¹³ photocatalytic oxidation and mineralization of wide range of organic dyes^{13,14,15}, pesticides.^{16,17} They have also been used for the photocatalytic reduction and recovery of toxic metal ions for their removal from aqueous solutions.^{18,19} However, the main disadvantages of POMs compounds is their high solubility and poor recyclability which limit their reuse as photocatalysts^{20,21} for organic pollutants removal from aqueous media. Many efforts have been devoted to overcome the POMs solubility such as combination with counter ion to give insoluble salt,²² impregnation on TiO₂²³ or silica gel²⁴ and immobilization onto active carbon.²⁵

In the present paper, we propose the POMs immobilization into polymer matrixes which can be useful to address reusability issues and introduce their photocatalytic properties into prepared composites that can be employed in continuous photocatalytic processes.

Therefore, we reported herein a simple method for the synthesis of (POM/polymer) composites based on polyoxometalates ($\text{H}_3\text{PMo}_{12}\text{O}_{40}$ and $\text{SiMo}_{12}\text{O}_{40}(\text{IPh}_2)_4$). These new composites have been prepared by photopolymerization under safe and eco-friendly visible light irradiation. The used POMs do not present significant absorption under visible light irradiation (see Figure 2A and Figure 2B) allowing the use of Light Emitting Diode LED@405nm for the composite synthesis by photopolymerization and consequently the preservation of the POM photocatalytic activity. Therefore, the polymeric matrix reported herein plays the role of host for the used POM which makes it more stable and overcomes its solubility in solution.

The photocatalytic activity of the new synthesized hybrid composites has been investigated for dye removal. Eosin-Y (EY), has been selected as a benchmarked dye which is widely used for medical applications, diagnosis purposes and biomedical research laboratories. It is toxic and mutagenic for human and animals.²⁶

2. Experimental section

2.1. Polyoxometalates and C11 synthesis

All reagents and solvents were purchased from Aldrich or Alfa Aesar and used as received without further purification. Mass spectroscopy was performed by the Spectropole of Aix-Marseille University. ESI mass spectral analyses were recorded with a 3200 QTRAP (Applied Biosystems SCIEX) mass spectrometer. The HRMS mass spectral analysis was performed with a QStar Elite (Applied Biosystems SCIEX) mass spectrometer. Elemental analyses were recorded with a Thermo Finnigan EA 1112 elemental analysis apparatus driven by the Eager 300 software. ^1H and ^{13}C NMR spectra were determined at room temperature in 5 mm o.d. tubes on a Bruker Avance 400 spectrometer of the Spectropole: ^1H (400 MHz) and ^{13}C (100 MHz). The ^1H chemical shifts were referenced to the solvent peak DMSO (2.49 ppm) and the ^{13}C chemical shifts were referenced to the solvent peak DMSO (49.5 ppm). All these carbazole photoinitiators were prepared with analytical purity up to accepted standards for new organic compounds (> 98%) which was checked by high field NMR analysis. 4-(*Bis*(4-bromophenyl)amino)benzaldehyde was synthesized as previously reported in the literature, without modifications and in similar yields [Haizhen Wang, Wenhui Ding, Gang Wang, Chunyue Pan, Meihong Duan, Guipeng Yu, J. APPL. POLYM. SCI. 2016, DOI: 10.1002/APP.44182]. $\text{H}_3\text{PMo}_{12}\text{O}_{40}$ [1] and $\text{SiMo}_{12}\text{O}_{40}(\text{IPh}_2)_4$ [2] were prepared according to the published procedures

[1]C. Rocchiccioli-Deltcheff ; M. Fournier ; R. Franck; R. Thouvenot *Inorg. Chem.*, **1983**, 22, 207-216

[2] JOURNAL OF POLYMER SCIENCE PART A-POLYMER CHEMISTRY 2015
Volume: 53 Issue: 8 Pages: 981-

Synthesis of 4-(bis(4-(naphthalen-1-yl)phenyl)amino)benzaldehyde

Tetrakis(triphenylphosphine)palladium (0) (0.46 g, 0.744 mmol) was added to a mixture of 4-(bis(4-bromophenyl)amino)benzaldehyde (2.52 g, 6.11 mmol), naphthalene-1-boronic acid (2.18 g, 12.66 mmol), toluene (54 mL), ethanol (26 mL) and an aqueous potassium carbonate solution (2 M, 6.91 g in 25 mL water, 26 mL) under vigorous stirring. The mixture was stirred at 80°C for 48 h under a nitrogen atmosphere. After cooling to room temperature, the reaction mixture was poured into water and extracted with ethyl acetate. The organic layer was washed with brine several times, and the solvent was then evaporated. Addition of dichloromethane followed by pentane precipitated a white solid which was filtered off. The residue was purified by column chromatography (SiO₂, pentane/DCM: 1/1 and pure DCM) and isolated as a solid (2.69 g, 84% yield). ¹H NMR (CDCl₃) δ: 7.26 (d, 2H, J = 8.7 Hz), 7.39 (d, 4H, J = 8.5 Hz), 7.46-7.57 (m, 12H), 7.80 (d, 2H, J = 8.7 Hz), 7.88 (d, 2H, J = 8.1 Hz), 7.93 (dd, 2H, J = 7.3 Hz, J = 1.8 Hz), 8.02 (d, 2H, J = 7.7 Hz), 9.89 (s, 1H); ¹³C NMR (CDCl₃) δ : 120.1, 125.4, 125.87, 125.93, 126.1, 127.0, 127.8, 128.4, 131.41, 131.44, 131.5, 132.0, 132.2, 133.9, 137.6, 139.4, 145.3, 153.3, 190.4; HRMS (ESI MS) m/z: theor: 525.2093 found: 525.2091 ([M]⁺ detected).

2.2. Other Chemical compounds

The monomer used for radical polymerization is trimethylol propane triacrylate (TMPTA) was purchased from Allnex. Bis(4-*tert*-butylphenyl)iodoniumhexafluorophosphate (Iod or Speedcure 938) and bis(2,4,6-trimethyl-benzoyl)phenylphosphine oxide (BAPO or speedcure BPO) were acquired from Lambson Ltd. Eosin-Y (Acid Red 87) and 2,2,6,6-tetramethyl-1-piperidinyloxy (TEMPO) were obtained from sigma Aldrich and 4-methoxyphenol (MEHQ) was obtained from Alfa Aesar. The chemical structure of the reagents used in this study is given by Figure 1.

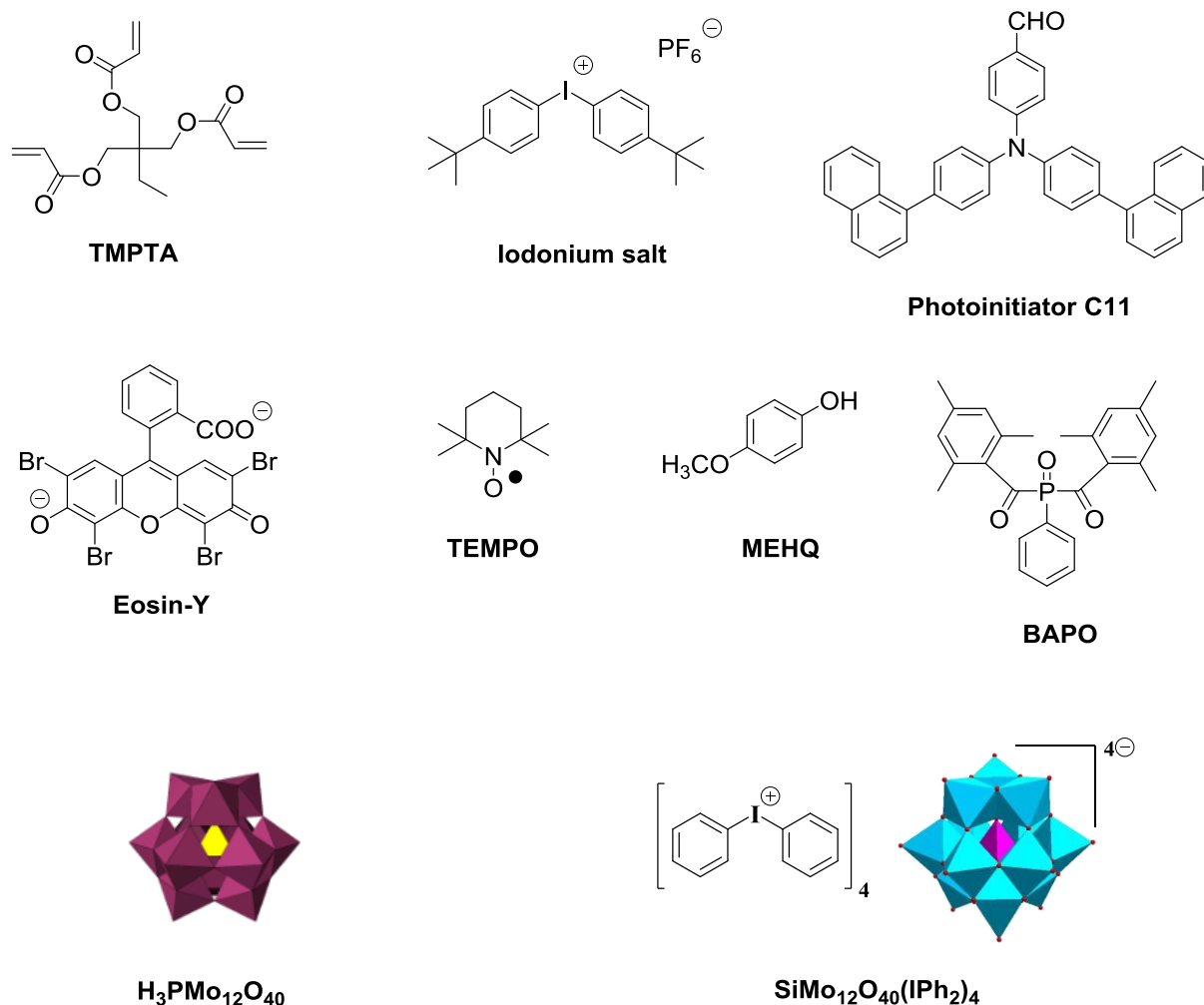


Figure 1: Chemical structures of the main compounds used in this work.

2.3. Irradiation sources:

As Light Emitting Diodes (LEDs), we used the following irradiation sources: LED@375 nm, $I_0 = 70 \text{ mW.cm}^{-2}$ and LED@405nm, $I_0 = 100 \text{ mW.cm}^{-2}$.

2.4. Photocatalysis experiments

The Eosin-Y samples were prepared by dissolving 10 mg in 1L of acetonitrile. The pH of the working solution was adjusted to 8 at which Eosin-Y is present under the form of its dianionic state.

When experiments were carried out in the presence of POM in solution, 1 mg of POM catalyst was added to the spectrophotometer cell in the presence of 4 ml of Eosin-Y (20 ppm) solution. When the experiment was carried out in the presence of composite POM/polymer, the prepared composite (pellet) was added directly to the EY solution. In all cases, monitoring of the Eosin-Y concentrations in solution over time was performed using a JASCO V730

spectrophotometer. The solutions were analyzed in a spectrophotometer cell with 1 cm path length and data were collected in absorbance mode.

3. Results and discussions

3.1. Study of Eosin-Y photolysis in the presence of POM in solution

The UV- vis absorption spectra of the studied POMs in acetonitrile were assessed. Figure 2.A and 2.B show that $H_3PMo_{12}O_{40}$ has an important UV absorption at 375 nm ($\epsilon_{375}= 4471,85 \text{ mol}^{-1} \cdot \text{L} \cdot \text{cm}^2$) compared to $SiMo_{12}O_{40}(IPh_2)_4$ ($\epsilon_{375}= 361 \text{ mol}^{-1} \cdot \text{L} \cdot \text{cm}^2$). Therefore, the LED@375nm will be used as an irradiation source to activate and exploit the photocatalytic properties of the POMs.

In order to study the photocatalytic activity of both POMs ($H_3PMo_{12}O_{40}$ and $SiMo_{12}O_{40}(IPh_2)_4$) on Eosin-Y removal efficiencies, the photolysis of the dye in acetonitrile solution with and without POM was firstly reported (Figure 2C).

The visible absorption spectra of Eosin-Y in acetonitrile in absence of POM at different irradiation times using LED@375 nm is shown in Figure 2C which indicates almost no temporal changes of the absorption peak observed at 532nm, assigned to the chromophore responsible for the solution color. This result indicates that the Eosin-Y is stable in acetonitrile upon the exposure to LED irradiation @375nm and did not decompose.

However, in the presence of the photocatalyst $H_3PMo_{12}O_{40}$, the absorption peak of EY in acetonitrile has completely disappeared just after 1 min of LED @375 nm (Figure 2D). In the case of $SiMo_{12}O_{40}(IPh_2)_4$ (Figure 2 E), the Eosin-Y peak disappeared after about 33 min using the same irradiation source. These relative fast photolysis in presence of the POMs confirm their ability in decomposing EY.

On the other hand, the photocatalytic activity of the studied POMs in comparison with titanium dioxide (TiO_2) under the same experimental conditions was studied. The experimental results indicate that in the presence of TiO_2 , no temporal change of the absorption peak of Eosin-Y using LED@375 nm (Figure 2F) was registered. This result could be explained by the fact that in basic media, the TiO_2 and EY are both negatively charged therefore the photodegradation is greatly inhibited since it occur on or near the TiO_2 surface.²⁷

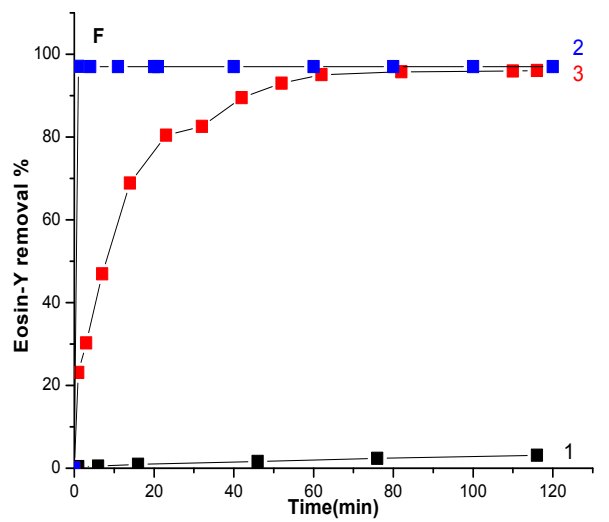
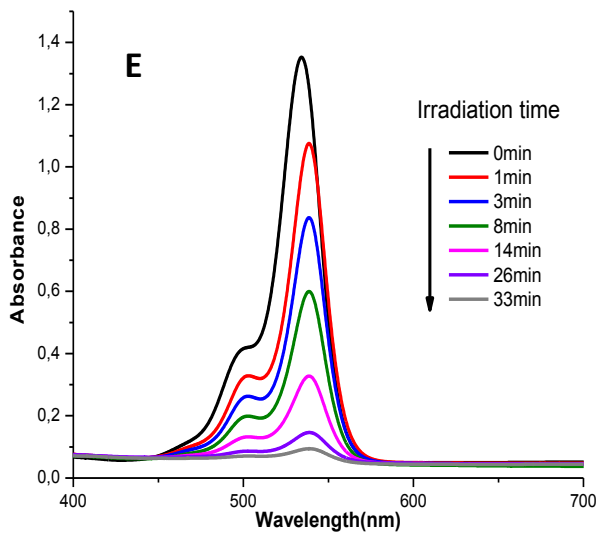
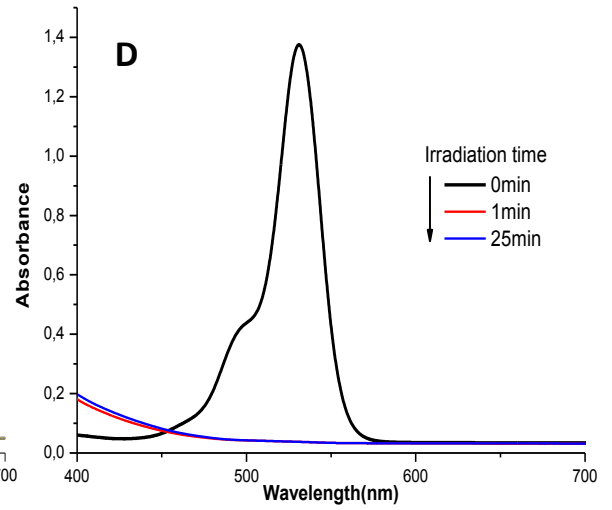
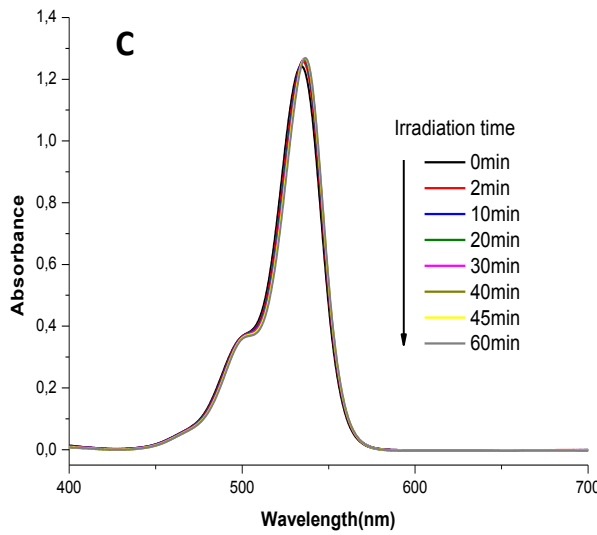
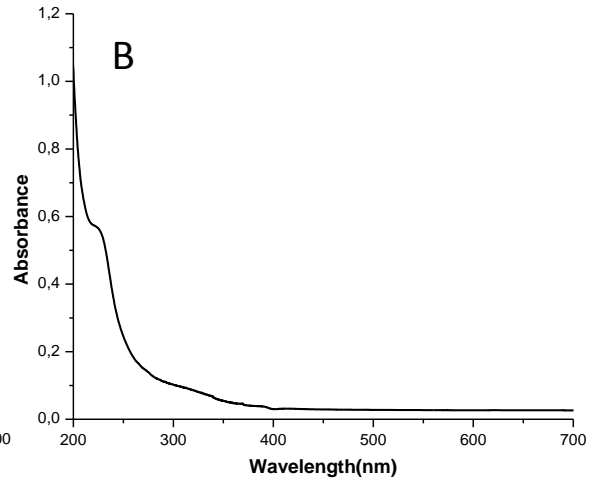
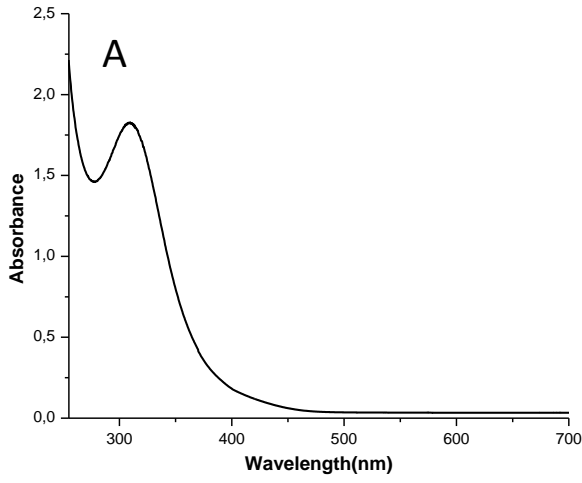


Figure 2.(A): UV-vis absorption spectra of $\text{H}_3\text{PMo}_{12}\text{O}_{40}$ (0.15 g.L^{-1}) in acetonitrile; (B): UV-vis absorption spectrum of $\text{SiMo}_{12}\text{O}_{40}(\text{IPh}_2)_4$ (0.25 g.L^{-1}) in acetonitrile; (C): UV-vis absorption spectra of Eosin-Y (20 mg.L^{-1}) in acetonitrile at different irradiation times (LED@375nm); (D): UV-vis absorption spectra of Eosin-Y (20 mg.L^{-1}) in acetonitrile at different irradiation times (LED@375nm) in the presence of $\text{H}_3\text{PMo}_{12}\text{O}_{40}$ (0.33 g.L^{-1}) in solution; (E): UV-vis absorption spectra of Eosin-Y (20 mg.L^{-1}) in acetonitrile at different irradiation time (LED@375nm) in the presence of $\text{SiMo}_{12}\text{O}_{40}(\text{IPh}_2)_4$ in solution and (F): Eosin-Y removal in the presence of (1) TiO_2 ; (2) $\text{H}_3\text{PMo}_{12}\text{O}_{40}$ and (3) $\text{SiMo}_{12}\text{O}_{40}(\text{IPh}_2)_4$.

The results shown in **Figure 2F** prove the efficiency of both polyoxometalates $\text{H}_3\text{PMo}_{12}\text{O}_{40}$ and $\text{SiMo}_{12}\text{O}_{40}(\text{IPh}_2)_4$ as photocatalysts for the degradation of Eosin-Y under near UV light (LED@375 nm) without additional chemical compounds such as H_2O_2 . Therefore, polyoxometalates are competitor photocatalysts to TiO_2 for organic dyes photodegradation especially when operating in mild conditions.

Since $\text{H}_3\text{PMo}_{12}\text{O}_{40}$ is soluble in water and the used solvent and $\text{SiMo}_{12}\text{O}_{40}(\text{IPh}_2)_4$ is used as suspension in the reaction media, we had difficulties while recovering the used POMs from the treated media. As a solution, POMs were immobilized into a polymer resin through a POM/polymer composite to ensure their reusability. The chosen resin polymer should be able not only to photopolymerize under visible light exposure but also to preserve the POMs photocatalytic activities after the synthesis process.

In the next sections, we detailed firstly the development of photosensitive resin for the composite POM/polymer synthesis under visible light and secondly the photocatalytic degradation of EY with the new **synthesized** POM/polymer composites.

3.2. Free radical polymerization of TMPTA under visible light irradiation

3.2.1. Free radical polymerization of TMPTA using a new photoinitiating system C11/Iod

The aim of this experimental part is to investigate the best photopolymerized formulation in terms of ratios of the used photoinitiator (C11) and conversion rate of the used monomer (TMPTA) under visible light irradiation LED@405nm in order to avoid the **deactivation** of the POMs. C11 was selected for its interesting absorption @405 nm and its reactivity with iodonium salt (Iod).

3.2.1.1. Light absorption properties of the studied photoinitiator

The ground state absorption spectrum of the proposed photoinitiator C11 in acetonitrile is reported in Figure 3. The molar extinction coefficient of C11 is about $3150 \text{ M}^{-1} \cdot \text{cm}^{-1}$ at 405 nm. The absorption spectra of C11 between 400-420 nm is quite interesting and overlaps with the emission spectra of LED@405 nm that will be used for the free radical polymerization of TMPTA.

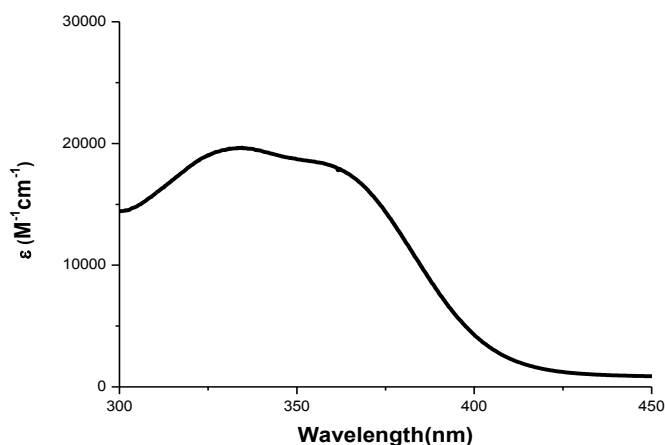


Figure 3: Absorption properties of C11 in acetonitrile.

3.2.1.2. Free radical polymerization of TMPTA under visible light irradiation

The double bond conversion can be clearly observed at 6165 cm^{-1} in the FTIR spectra (Figure 4A). In fact, upon LED@405 irradiation, the free radical polymerization (FRP) of TMPTA using the couple C11/Iod (0.5%/1%/w/w) has an interesting conversion of 35% after only 100 s of light exposure. This result is encouraging and could be improved by changing the C11 content. Therefore, as depicted in Figure 4B the most effective ratio of the couple C11/Iod is: 0.1%/1% w/w which efficiently initiates the polymerization of TMPTA under air and leads to a high final conversion of about 65% for only 100s of visible light irradiation using LED@405 nm. This result could be explained by the fact that the used photoinitiator C11 absorbs under 405 nm leading to an inner filter effect for high content decreasing the TMPTA conversion.

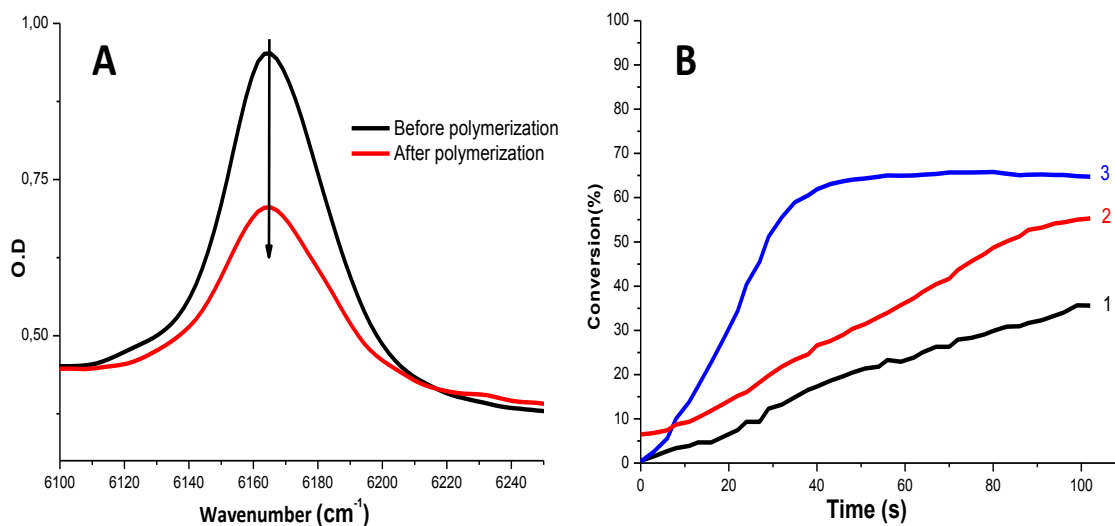


Figure 4.(A): **Near** Infrared spectra recorded before and after polymerization of TMPTA using C11/Iod (0.1%/1% w/w) under LED irradiation @405nm; (B): Photopolymerization profiles of double bond conversion vs irradiation time upon the exposure to LED@405nm in the presence of various ratios of the system (C11/Iod) (1): 0.5% **C11/1% Iod**; (2): 0.3% **C11/1 %Iod** and (3): **0.1% C11/1% Iod**.

3.2.1.3. Free radical polymerization of TMPTA using a commercial photoinitiator

The photopolymerization of TMPTA using BAPO, known as a commercial photoinitiator, in the presence of Iodonium salt was studied in order to make the photopolymerization process easier and more efficient. The conversion of the double bond of TMPTA is more important than the case of the couple (C11-Iod), reaching 80% after only **50 s** of LED@405nm irradiation (Figure 5).

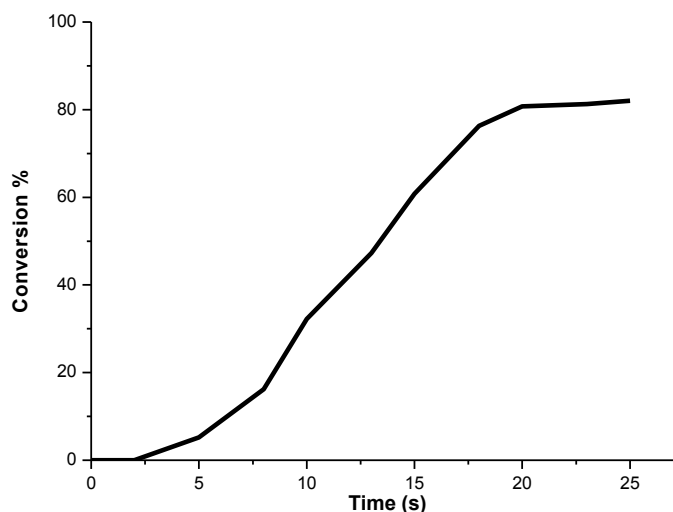


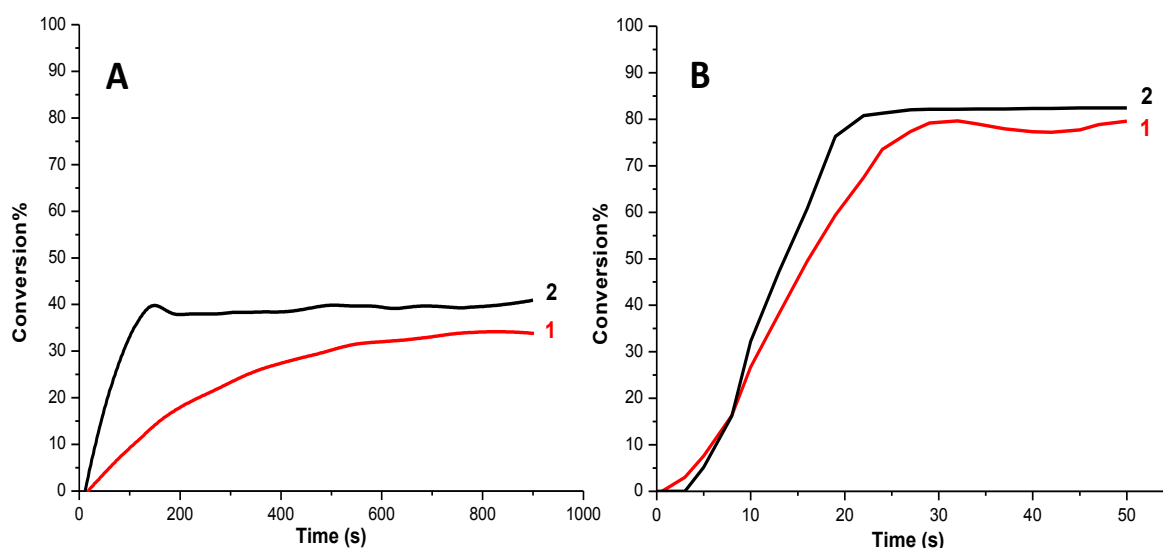
Figure 5: Photopolymerization profile of double bond conversion vs irradiation time upon the exposure to LED@405nm in the presence of the system BAPO/Iod (0.2%/1% w/w).

Comparing the double bond of conversion of TMPTA using the system (C11/Iod) (Figure 4 B curve 3) and (BAPO-Iod) (Figure 5), the commercial photoinitiator seems to be more efficient in terms of both conversion and irradiation time (82% in 20s vs. 65% in 100s).

Therefore, the developed photosensitive formulation can be interesting to host the studied POMs in order to synthesize hybrid POM/polymer composites for photocatalytic applications.

3.3. Synthesis of the hybrid POM/polymer composite

Figure 6 shows that these new POM/polymer composites can be prepared by photopolymerization with an excellent photopolymerization profile. Indeed Figure 6A (curve 1) indicates that the system $\text{H}_3\text{PMo}_{12}\text{O}_{40}$ (0.3% w/w), C11/Iod (0.1%/0.5%/w/w) in TMPTA polymerizes under air upon visible light exposure using LED@405nm and leads to about 38% as final conversion acrylate function conversion. Figure 6 A (curve 2) shows that the system $\text{SiMo}_{12}\text{O}_{40}(\text{IPh}_2)_4$ (1.12% w/w), C11/Iod (0.1%/0.5%/w/w) in TMPTA is also efficiently polymerized upon visible light exposure using the same source of irradiation leading to a high double bond conversion of about 39% after 300s of irradiation under air.



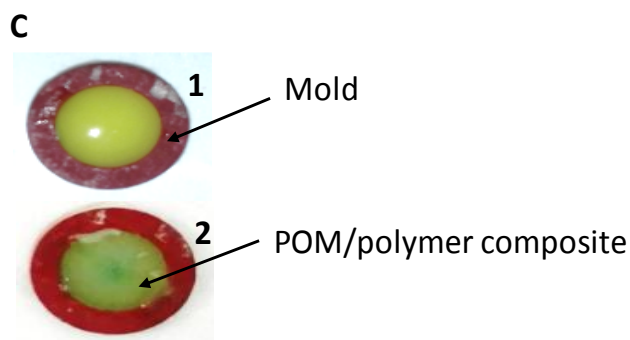


Figure 6.(A): Photopolymerization profiles of TMPTA (acrylate conversion vs irradiation time) under air, upon the exposure to LED@405nm in the presence of (1) $\text{H}_3\text{PMo}_{12}\text{O}_{40}$ (0.3% w/w), C11 (0.1% w/w) and Iod (0.5% w/w) and (2) $\text{SiMo}_{12}\text{O}_{40}(\text{IPh}_2)_4$ (1.13%w/w), C11 (0.1% w/w) and Iod (0.5% w/w); (B): Photopolymerization profiles of TMPTA (acrylate conversion vs irradiation time) under air, upon the exposure to LED@405nm in the presence of (1) $\text{H}_3\text{PMo}_{12}\text{O}_{40}$ (1.13% w/w), BAPO (0.3% w/w) and Iod (1% w/w) and (2) $\text{SiMo}_{12}\text{O}_{40}(\text{IPh}_2)_4$ (1.13% w/w), BAPO (0.2% w/w) and Iod (1% w/w) and (C) Pellet of POM/polymer composite (1): before polymerization and (2) after polymerization.

On the other hand, the photopolymerization of the systems using BAPO is still more efficient under visible light irradiation in terms of acrylate final conversion: 80% after only 30s of irradiation in the case of $\text{H}_3\text{PMo}_{12}\text{O}_{40}$ (1.3% w/w), BAPO-Iod (0.2%/1% w/w) (Figure 6 B (curve1)) and about 90% after only 20s in the case of $\text{SiMo}_{12}\text{O}_{40}(\text{IPh}_2)_4$ (1.3% w/w), BAPO-Iod (0.2%/1% w/w) (Figure 6B (curve2)).

Thus, new photosensitive systems (POM, C11, Iod) and (POM, BAPO, Iod) were developed able to polymerize TMPTA efficiently under mild visible light irradiation to obtain POM/Polymer composites without detrimental effect on the polymerization kinetics for the presence of the studied POMs: $\text{H}_3\text{PMo}_{12}\text{O}_{40}$ and $\text{SiMo}_{12}\text{O}_{40}(\text{IPh}_2)_4$.

4. Photocatalytic activity of the new hybrid POM/Polymer composites

The synthesis of new composites using a polymer matrix as a host for the used inorganic catalyts $\text{H}_3\text{PMo}_{12}\text{O}_{40}$ and $\text{SiMo}_{12}\text{O}_{40}(\text{IPh}_2)_4$ and their photocatalytic ability on Eosin-Y removal was studied under UV irradiation. These experiments were carried in the presence of the synthesized composite without the addition of any other chemical oxidant using the LED@375 nm. The obtained absorption spectra of Eosin-Y are reported in Figure 7 and 8 for different irradiation times.

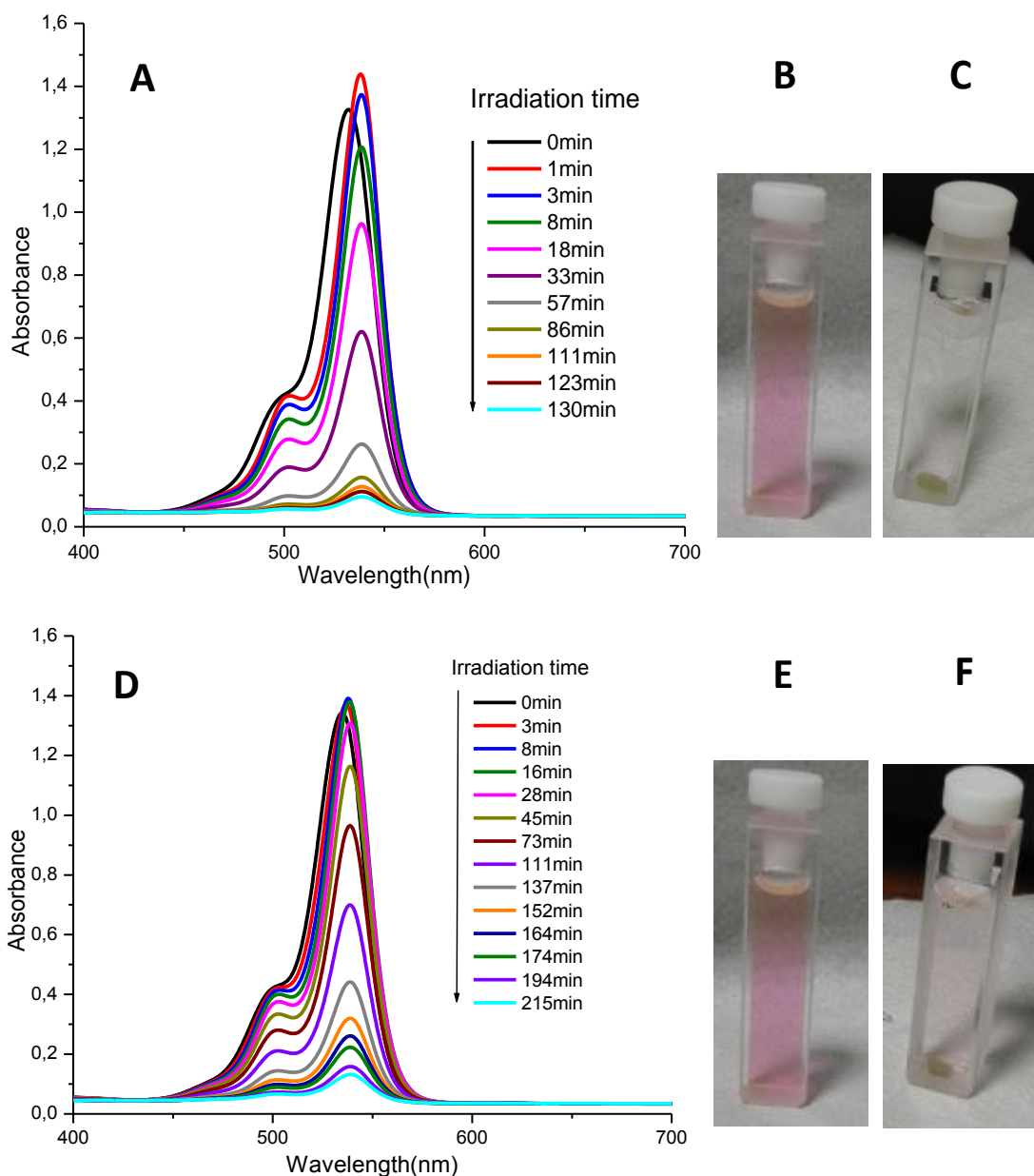


Figure 7. (A): UV-vis absorption spectra of Eosin-Y (20 ppm) in acetonitrile at different irradiation time upon LED@375nm in the presence of composite $H_3PMo_{12}O_{40}$ /polymer (C11/Iod) photopolymerized under air; (B):Eosin-Y in acetonitrile before photodegradation; (C): Eosin-Y in acetonitrile after photodegradation in the presence of the composite $H_3PMo_{12}O_{40}$ /polymer (C11/Iod); (D): UV-vis absorption spectra of Eosin-Y (20 ppm) in acetonitrile at different irradiation time of LED@375nm in the presence of composite $SiMo_{12}O_{40}(IPh_2)_4$ /polymer (C11/Iod) photopolymerized under air; (E):Eosin-Y in acetonitrile before photodegradation and (F): Eosin-Y in acetonitrile after photodegradation in the presence of the composite $SiMo_{12}O_{40}(IPh_2)_4$ /polymer (C11/Iod).

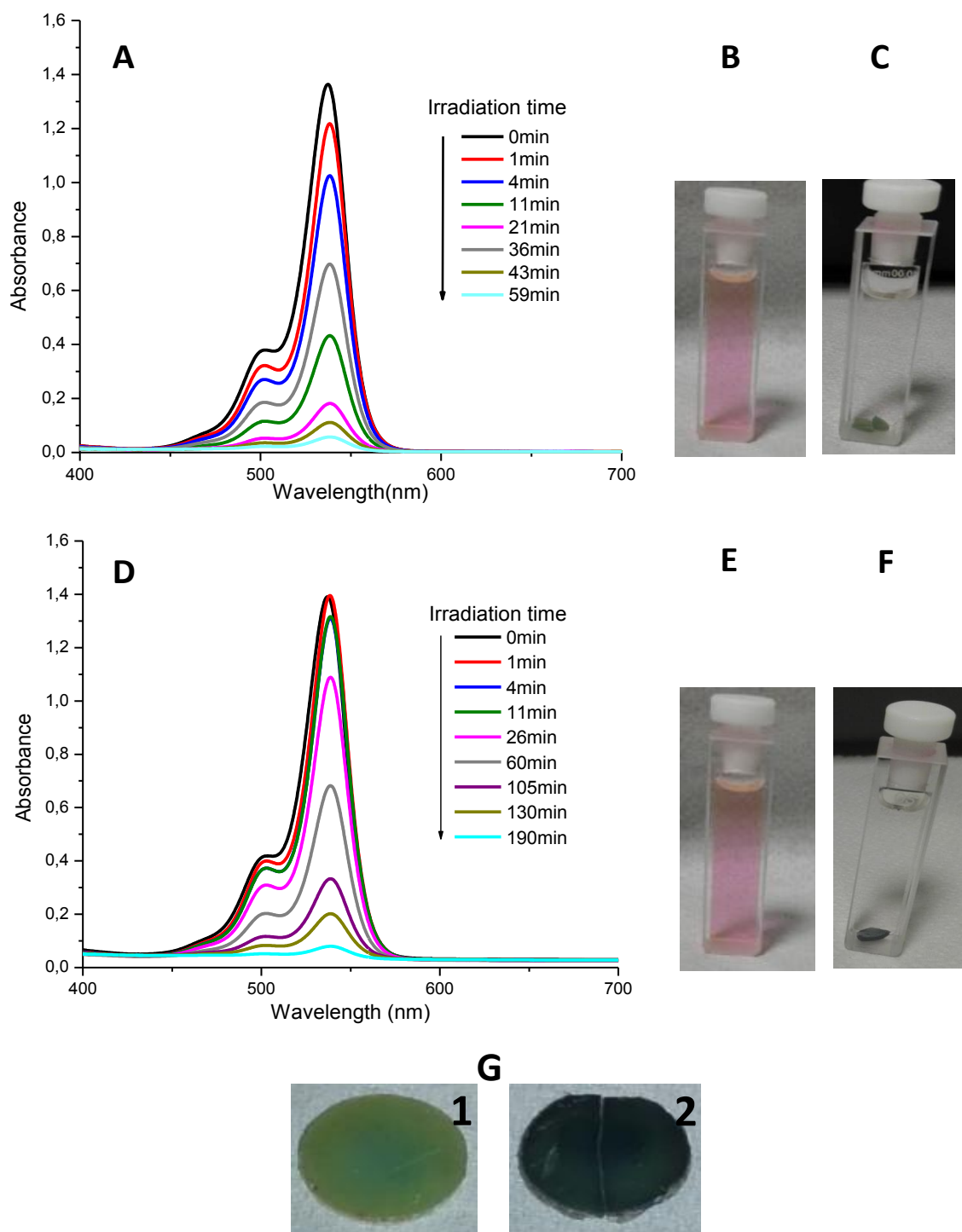
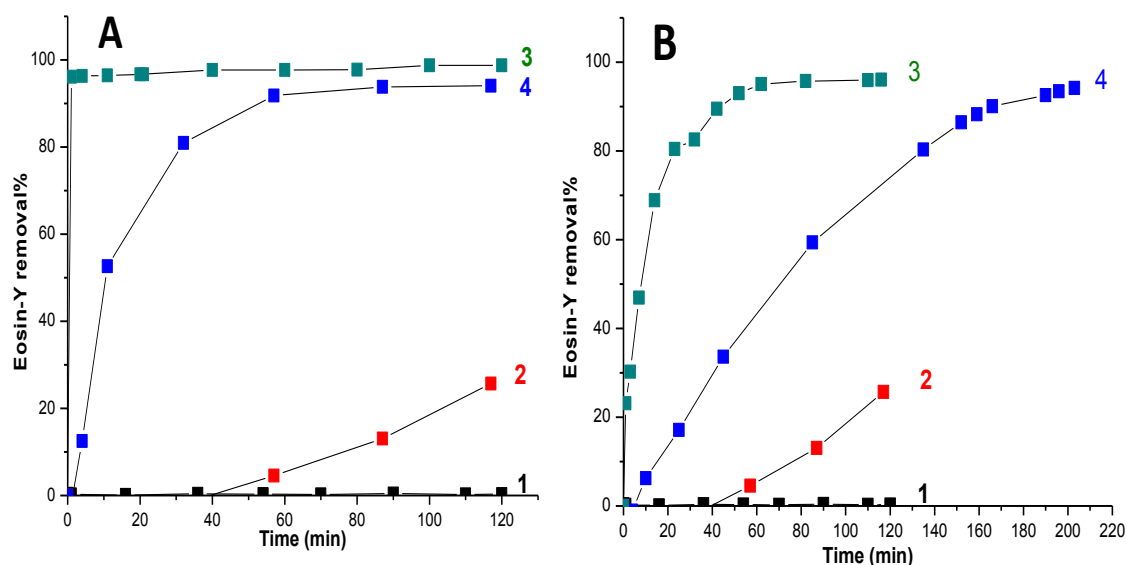


Figure 8. (A): UV-vis absorption spectra of Eosin-Y (20 ppm) in acetonitrile at different irradiation time of LED@375nm in the presence of $H_3PMo_{12}O_{40}$ /polymer (BAPO-Iod) composite photopolymerized under air; (B): Eosin-Y in acetonitrile before photodegradation; (C): Eosin-Y in acetonitrile after photodegradation in the presence of the composite $H_3PMo_{12}O_{40}$ /polymer (BAPO-Iod); (D): UV-vis absorption spectra of Eosin-Y (20 ppm) in acetonitrile at different irradiation time of LED@375nm in the presence of composite $SiMo_{12}O_{40}(IPh_2)_4$ /polymer(BAPO-Iod) photopolymerized under air; (E): Eosin-Y in acetonitrile before photodegradation; (F): Eosin-Y in

acetonitrile after photodegradation in the presence of the composite $\text{SiMoO}_{12}\text{O}_{40}(\text{IPh}_2)_4$ /polymer (BAPO-Iod) and (G): Example of POM/polymer (BAPO-Iod) composite: (1) Before Photolysis and (2) after Photolysis.

Figure 7 and show that the absorption peaks of Eosin-Y were gradually reduced in line with increasing the irradiation time using LED@375nm in the presence of each of the composites ($\text{H}_3\text{PMO}_{12}\text{O}_{40}$ /polymer or $\text{SiMoO}_{12}\text{O}_{40}(\text{IPh}_2)_4$ /polymer). This behavior indicates the net discoloration of the Eosin-Y solutions after the photolysis.

As blank experiment, we realized the photolysis of Eosin-Y in acetonitrile in the presence of polymers without POMs obtained by photopolymerization of TMPTA with C11/Iod (0.1%/0.5%/w/w) (Figure 9A (curve 2) and Figure 9B (curve 2)) or BAPO-Iod (0.2%/1%/w/w) (Figure 9C (curve 2) and Figure 9D (curve 2)). These reference polymers are prepared in the same condition as the photopolymerization of the composite POM/polymer using LED@405nm as irradiation source. The conversion of Eosin-Y versus reaction time under different conditions was reported in Figure 9.



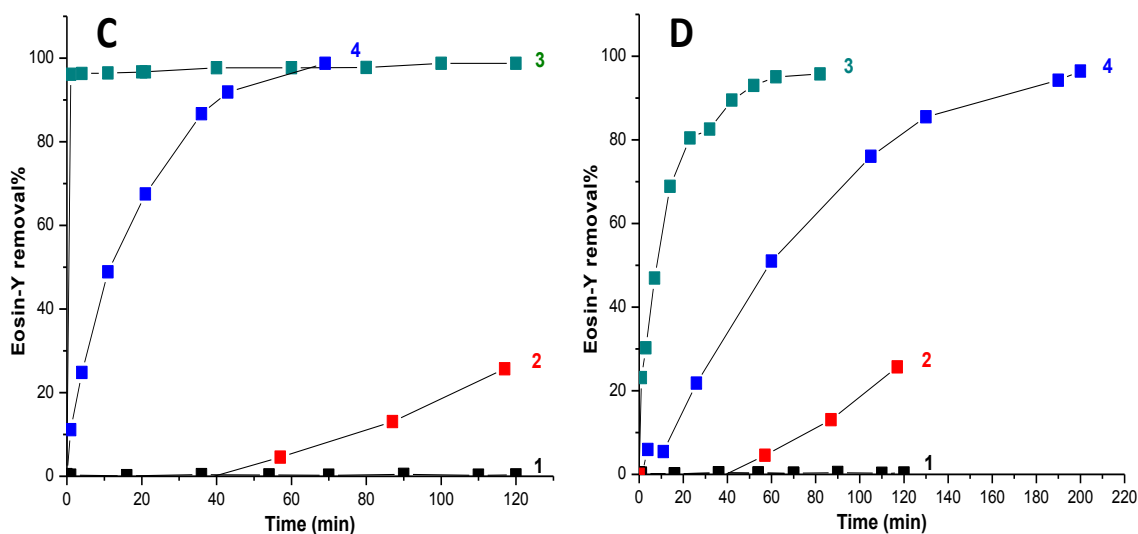


Figure 9.(A): Conversion of Eosin-Y under LED Irradiation @375nm (1): without composite; (2): in the presence of pellet of Polymer C11/Iod (0.1%/0.5% /w/w) without POM; (3): in the presence of $H_3PMo_{12}O_4$ in solution; (4): in the presence of composite ($H_3PMo_{12}O_4$ (0.3% w/w)/polymer) (C11/Iod (0.1%/0.5% /w/w)); (B): conversion of Eosin-Y under LED Irradiation @375nm (1): without composite; (2): in the presence of pellet of Polymer C11/Iod (0.1%/0.5%/w/w) without POM; (3): in the presence of $SiMo_{12}O_{40}(IPh_2)_4$ in solution and (4): in the presence of ($SiMo_{12}O_{40}(IPh_2)_4$ (1% w/w) /polymer) (C11/Iod (0.1%/0.5% /w/w)); (C): Conversion of Eosin-Y under LED Irradiation @375nm: (1) without composite; (2): In the presence of pellet of Polymer (BAPO-Iod (0.2%/1% /w/w)) without POM; (3): in the presence of $H_3PMo_{12}O_4$ in solution; (4): in the presence of ($H_3PMo_{12}O_4$ (1.3% w/w)/polymer) (BAPO-Iod (0.2%/1% /w/w)) composite and (D) conversion of Eosin-Y under LED Irradiation @375nm (1): without composite; (2): In the presence of pellet of Polymer (BAPO-Iod (0.2%/1% /w/w)) without POM; (3): in the presence of $SiMo_{12}O_{40}(IPh_2)_4$ in solution and (4): in the presence of ($SiMo_{12}O_{40}(IPh_2)_4$ (1.3% w/w) /polymer) (BAPO-Iod (0.2%/1% /w/w)) composite.

Figure 9A (curve 4) shows that the $H_3PMo_{12}O_4$ /polymer (C11/Iod) composite is more efficient photocatalyst than $SiMo_{12}O_{40}(IPh_2)_4$ /polymer (C11/Iod) (figure 9B (curve 4)) since the EY removal reached respectively 93% after only 87 min vs 200min of LED@375nm irradiation. In contrast, it is only 26% after 117 min in the presence of the reference polymer (C11/Iod) without POM (figure 9 (curves 2)) and 1% in the case of EY without composite (Figure 9 (curves 1)).

In the same line, Figure 9D (curve 4) shows that Eosin-Y is almost totally removed (98% after 60 min of irradiation) in the presence of the composite $H_3PMo_{12}O_4$ /polymer (BAPO-Iod). Also, in the case of composite $SiMo_{12}O_{40}(IPh_2)_4$ /polymer (BAPO-Iod) (Figure 9.C (curve 4) the Eosin-Y removal is about 94% after 190 min of irradiation. This result goes with

the Eosin removal in the case of $\text{SiMo}_{12}\text{O}_{40}(\text{IPh}_2)_4$ /polymer (C11/Iod) (see figure 9B (curve 4) since the two composites have the same amount of $\text{SiMo}_{12}\text{O}_{40}(\text{IPh}_2)_4$ (1%).

In all cases, by comparing the Eosin-Y removal in the presence of the reference polymers without POMs (Figure 9 (curves 2)), with its removal in the presence of POM/polymer composites (Figure 9 (curves 4)), we can obviously distinguish the photocatalytic activity of the immobilized POMs in the polymer on the Eosin-Y removal.

Indeed, these results prove that the POMs encapsulated in the polymer keep their catalytic activity under UV irradiation and therefore their effectiveness for Eosin-Y removal capacities. Besides, the composite $\text{H}_3\text{PMo}_{12}\text{O}_{40}$ /polymer (BAPO-Iod) (Figure 9C (curve 4)) and the composite $\text{H}_3\text{PMo}_{12}\text{O}_{40}$ /polymer (C11/Iod) (Figure 9A (curve 4)) had nearly the same behavior for Eosin-Y removal despite the difference of the used amount of $\text{H}_3\text{PMo}_{12}\text{O}_{40}$ respectively (1.13% and 0.3%) which demonstrates the relatively high efficiency of $\text{H}_3\text{PMo}_{12}\text{O}_{40}$ as photocatalyst for organic dye removal.

After the photodegradation study of Eosin-Y in acetonitrile, its removal from aqueous solutions in the presence of the composite $\text{H}_3\text{PMo}_{12}\text{O}_{40}$ (1.3% w/w)/polymer (BAPO-Iod (0.2%/1% w/w)) under LED@375nm irradiation. Interestingly, as the first result, the experiment demonstrates its color removal (figure 10) which prove the efficiency of the synthesized composites POM/polymer as photocatalyst for organic dye removal from aqueous solutions also.

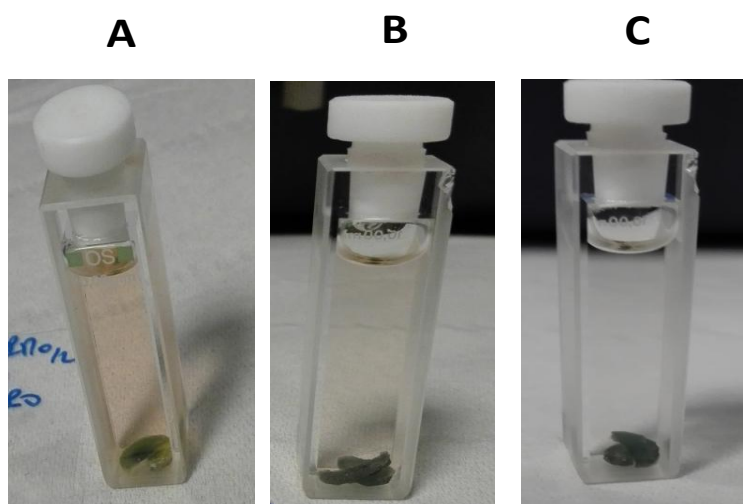


Figure 10: Example of Eosin-Y (20 ppm) photodegradation in water in the presence of the composite $\text{H}_3\text{PMo}_{12}\text{O}_4$ /polymer (BAPO-Iod) (A): Before irradiation; (B): after 100min of irradiation and (C) after 5h of irradiation.

5. Effect of atmosphere or scavenger agents on the photocatalytic mechanism

Other series of experiments were carried out to probe the mechanisms involved in the degradation of Eosin-Y in the presence of the new photocatalysts POM/Polymer under near UV irradiation. Experiments were conducted upon different atmosphere: under air, N₂ as well as some radicals scavengers (such as MEHQ for oxygenated radicals (RO[•] and ROO[•]) quencher²⁸, TEMPO for carbon centered radical quencher and isopropyl alcohol as (OH[•]) quencher (Figure 11).²⁹

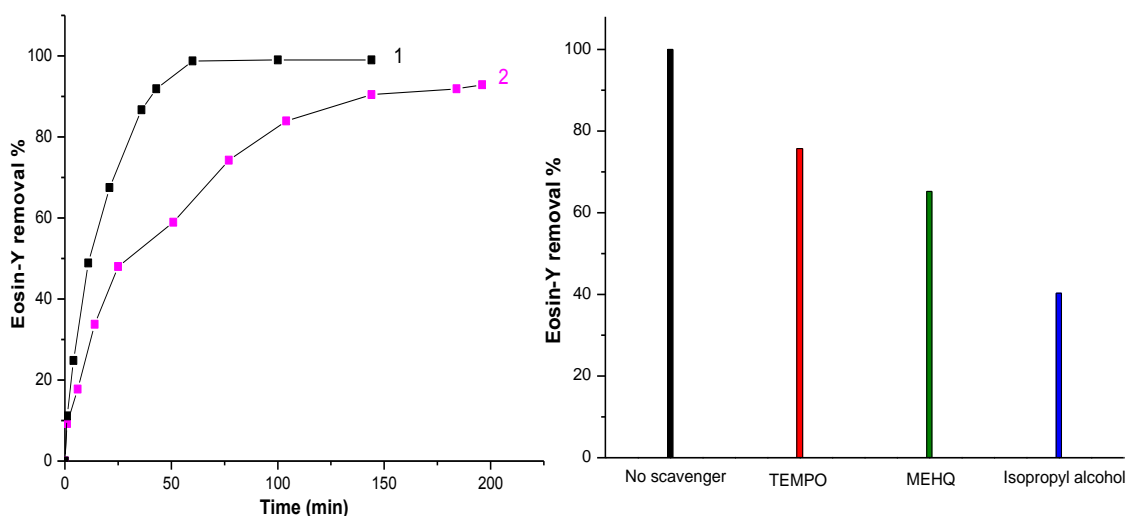


Figure 11. (A): Eosin-Y (20 ppm) removal in acetonitrile under LED Irradiation @375nm in the presence of composite H₃PMo₁₂O₄₀ (1.3% w/w)/polymer (BAPO-Iod (0.3%/1% /w/w)) under: (1) oxic media (2) anoxic media and; (B): Eosin-Y (20 ppm) removal in acetonitrile in the presence of composite H₃PMo₁₂O₄₀ (1.3% w/w)/polymer (BAPO-Iod (0.3%/1% /w/w)) after 2h of irradiation in the presence of scavengers: TEMPO (1mM), MEHQ (1mM) and isopropyl alcohol (10mM).

As shown in Figure 11, the atmosphere and the presence of scavenger agents have significant effects on the kinetic of degradation of Eosin-Y in the presence of the photocatalyst.

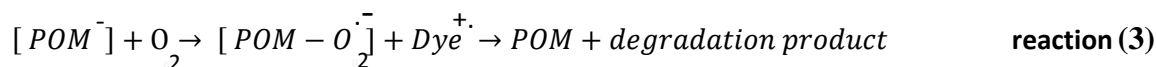
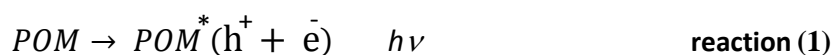
It is clear that the degradation rate under air is higher than under N₂ atmosphere (Figure 11A), this result illustrates two important points: i) the dissolved oxygen has a clear enhancing effect on the kinetic and the percentage of Eosin-Y removal, and ii) the ability of the photocatalyst to react directly with the adsorbed dye under anoxic conditions since the Eosin-Y removal reached 90% after 144 min of irradiation (Figure 11A (curve 2)). Therefore, an important part of the degradation mechanism is based on the activity of the POM composite under light irradiation. This is obvious also by the color change of the synthesized

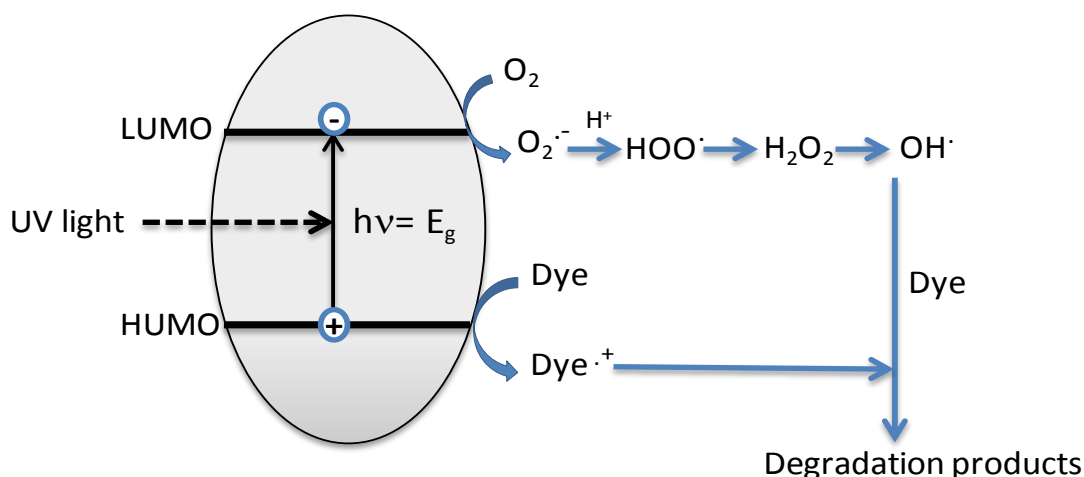
composites before and after photodegradation of Eosin-Y as seen in Figure 8G. Actually, the blue color of the composite after photodegradation is attributed to a change of the oxidation degree of the POM⁸ when encapsulated in the polymer matrix.

Figure 11B, shows that the kinetic of photodegradation is slower in the presence of some scavengers indicating that the generated radicals play also a key role in the photodegradation process. Actually, the obtained results suggest that the hydroxyl oxide (OH[•]) is the foremost responsible radical in the Eosin-Y degradation. MEHQ impedes also the degradation of Eosin-Y which could be attributed to a reaction between the generated oxygenated radicals (RO[•] and ROO[•]) with MEHQ which produce less reactive radicals and therefore lower efficiency for EY removal.

Based on the previously reported mechanisms^{30,11} and the above experimental results, the proposed mechanism (scheme 1) for the dye photodegradation can be described:

- i. The near UV light induces the excitation of POM which promote electron and hole separation¹¹ (reaction (1)).
- ii. These excited states (POM*) are powerful redox agent able to oxidize directly the adsorbed dye on its surface (reaction (2)) or react with other electron donor such as the adsorbed O₂ to produce oxidizing species (O₂^{•-}) and (OH[•]).
- iii. These latter radicals can attack the target organic dye resulting in its degradation (reaction (3)).





Schema 1: Proposed mechanism for the dye photodegradation when using Polyoxometalates as photocatalyst

6. Conclusion

In this work, an innovative research work regarding the synthesis and an environmental application for a green **composite** material was performed. It is based on the incorporation of polyoxometalates into polymeric matrix photopolymerized under visible light. The developed photosensitive resin **preserves** the photocatalytic properties of the studied POMs after photopolymerization. The immobilization of POMs into organic solid led to hybrid material with an efficient photocatalytic activity for Eosin-Y removal from both acetonitrile and aqueous solutions under near UV **irradiation**. **The** composite could be then easily recovered and recycled which fulfills an urgent demand for the industrial water treatment processes. This new material will offer new possibilities to strength the photocatalytic removal of organic contaminants from industrial effluents. Further investigations are currently undertaken in order to study the removal of other emergent pollutants from aqueous media.

Acknowledgments

Financial support from the Hubert Curien Utique Partnership (PHC-UTIQUE 2018 (code 18G1210)) of inter-university French-Tunisian scientific cooperation and the Ministry of Higher Education and Scientific Research (MERSRS) of Tunisia.

References

- (1) Gupta, V. K.; Jain, R.; Nayak, A.; Agarwal, S.; Shrivastava, M. Removal of the Hazardous Dye—Tartrazine by Photodegradation on Titanium Dioxide Surface. *Materials Science and Engineering: C* **2011**, *31* (5), 1062–1067. <https://doi.org/10.1016/j.msec.2011.03.006>.
- (2) Forgacs, E.; Cserháti, T.; Oros, G. Removal of Synthetic Dyes from Wastewaters: A Review. *Environment International* **2004**, *30* (7), 953–971. <https://doi.org/10.1016/j.envint.2004.02.001>.
- (3) Jassal, V.; Shanker, U.; Kaith, B. S. Aegle Marmelos Mediated Green Synthesis of Different Nanostructured Metal Hexacyanoferrates: Activity against Photodegradation of Harmful Organic Dyes. *Scientifica* **2016**, *2016*, 1–13. <https://doi.org/10.1155/2016/2715026>.
- (4) Javier Benitez, F.; Acero, J. L.; Real, F. J. Degradation of Carbofuran by Using Ozone, UV Radiation and Advanced Oxidation Processes. *Journal of Hazardous Materials* **2002**, *89* (1), 51–65. [https://doi.org/10.1016/S0304-3894\(01\)00300-4](https://doi.org/10.1016/S0304-3894(01)00300-4).
- (5) Rajeshwar, K.; Osugi, M. E.; Chanmanee, W.; Chenthamarakshan, C. R.; Zanoni, M. V. B.; Kajitvichyanukul, P.; Krishnan-Ayer, R. Heterogeneous Photocatalytic Treatment of Organic Dyes in Air and Aqueous Media. *Journal of Photochemistry and Photobiology C: Photochemistry Reviews* **2008**, *9* (4), 171–192. <https://doi.org/10.1016/j.jphotochemrev.2008.09.001>.
- (6) Sahel, K.; Perol, N.; Chermette, H.; Bordes, C.; Derriche, Z.; Guillard, C. Photocatalytic Decolorization of Remazol Black 5 (RB5) and Procion Red MX-5B—Isotherm of Adsorption, Kinetic of Decolorization and Mineralization. *Applied Catalysis B: Environmental* **2007**, *77* (1–2), 100–109. <https://doi.org/10.1016/j.apcatb.2007.06.016>.
- (7) Hiskia, A.; Papaconstantinou, E. Photocatalytic Oxidation of Organic Compounds by Polyoxometalates of Molybdenum and Tungsten. Catalyst Regeneration by Dioxygen. *Inorganic Chemistry* **1992**, *31* (2), 163–167. <https://doi.org/10.1021/ic00028a007>.
- (8) Papaconstantinou, E. Photochemistry of Polyoxometallates of Molybdenum and Tungsten and/or Vanadium. *Chemical Society Reviews* **1989**, *18*, 1. <https://doi.org/10.1039/cs9891800001>.
- (9) *Polyoxometalate Molecular Science: Proceedings of the NATO Advanced Study Institute on Polyoxometalate Molecular Science, Tenerife, Spain, 25 August - 4 September 2001*; Borrás-Almenar, J. J., Muller, A., Pope, M., Coronado, E., Eds.; NATO science series 2, Mathematics, physics and chemistry; Kluwer Acad. Publ: Dordrecht, 2003.
- (10) Pope, M. T.; Müller, A. *Polyoxometalate Chemistry from Topology via Self-Assembly to Applications*; Kluwer Academic Publishers: New York, 2001.
- (11) Hiskia, A.; Mylonas, A.; Papaconstantinou, E. Comparison of the Photoredox Properties of Polyoxometallates and Semiconducting Particles. *Chemical Society Reviews* **2001**, *30* (1), 62–69. <https://doi.org/10.1039/a905675k>.
- (12) Sadakane, M.; Steckhan, E. Electrochemical Properties of Polyoxometalates as Electrocatalysts. *Chem. Rev.* **1998**, *98* (1), 219–238. <https://doi.org/10.1021/cr960403a>.
- (13) Omwoma, S.; Gore, C. T.; Ji, Y.; Hu, C.; Song, Y.-F. Environmentally Benign Polyoxometalate Materials. *Coordination Chemistry Reviews* **2015**, *286*, 17–29. <https://doi.org/10.1016/j.ccr.2014.11.013>.
- (14) Liu, C.-G.; Zheng, T.; Liu, S.; Zhang, H.-Y. Photodegradation of Malachite Green Dye Catalyzed by Keggin-Type Polyoxometalates under Visible-Light Irradiation: Transition Metal Substituted Effects. *Journal of Molecular Structure* **2016**, *1110*, 44–52. <https://doi.org/10.1016/j.molstruc.2016.01.015>.
- (15) Okuhara, T.; Mizuno, N.; Misono, M. Catalytic Chemistry of Heteropoly Compounds. In *Advances in Catalysis*; Elsevier, 1996; Vol. 41, pp 113–252. [https://doi.org/10.1016/S0360-0564\(08\)60041-3](https://doi.org/10.1016/S0360-0564(08)60041-3).
- (16) Rafqah, S.; Chung, P. W.-W.; Forano, C.; Sarakha, M. Photocatalytic Degradation of Methylsulfuron Methyl in Aqueous Solution by Decatungstate Anions. *Journal of Photochemistry and Photobiology A: Chemistry* **2008**, *199* (2–3), 297–302. <https://doi.org/10.1016/j.jphotochem.2008.06.012>.

- (17) Texier, I.; Giannotti, C.; Malato, S.; Richter, C.; Delaire, J. Solar Photodegradation of Pesticides in Water by Sodium Decatungstate. *Catalysis Today* **1999**, 11.
- (18) Troupis, A.; Hiskia, A.; Papaconstantinou, E. Selective Photocatalytic Reduction–Recovery of Palladium Using Polyoxometallates. *Applied Catalysis B: Environmental* **2004**, 52 (1), 41–48. <https://doi.org/10.1016/j.apcatb.2004.02.016>.
- (19) Troupis, A.; Gkika, E.; Hiskia, A.; Papaconstantinou, E. Photocatalytic Reduction of Metals Using Polyoxometallates: Recovery of Metals or Synthesis of Metal Nanoparticles. *Comptes Rendus Chimie* **2006**, 9 (5–6), 851–857. <https://doi.org/10.1016/j.crci.2005.02.041>.
- (20) Costentin, C.; Evans, D. H.; Robert, M.; Savéant, J.-M.; Singh, P. S. Electrochemical Approach to Concerted Proton and Electron Transfers. Reduction of the Water–Superoxide Ion Complex. *Journal of the American Chemical Society* **2005**, 127 (36), 12490–12491. <https://doi.org/10.1021/ja053911n>.
- (21) Ozer, R. R.; Ferry, J. L. Photocatalytic Oxidation of Aqueous 1,2-Dichlorobenzene by Polyoxometalates Supported on the NaY Zeolite. *The Journal of Physical Chemistry B* **2002**, 106 (16), 4336–4342. <https://doi.org/10.1021/jp0138126>.
- (22) Neumann, R.; Levin, M. Selective Aerobic Oxidative Dehydrogenation of Alcohols and Amines Catalyzed by a Supported Molybdenum–Vanadium Heteropolyanion Salt Na₅PMo₂V₂O₄₀. *The Journal of Organic Chemistry* **1991**, 56 (19), 5707–5710. <https://doi.org/10.1021/jo00019a047>.
- (23) Ozer, R. R.; Ferry, J. L. Investigation of the Photocatalytic Activity of TiO₂–Polyoxometalate Systems. *Environmental Science & Technology* **2001**, 35 (15), 3242–3246. <https://doi.org/10.1021/es0106568>.
- (24) Guo, Y.; Wang, Y.; Hu, C.; Wang, Y.; Wang, E.; Zhou, Y.; Feng, S. Microporous Polyoxometalates POMs/SiO₂: Synthesis and Photocatalytic Degradation of Aqueous Organochlorine Pesticides. 8.
- (25) Izumi, Y.; Urabe, K. CATALYSIS OF HETEROPOLY ACIDS ENTRAPPED IN ACTIVATED CARBON. *Chemistry Letters* **1981**, 10 (5), 663–666. <https://doi.org/10.1246/cl.1981.663>.
- (26) Carson, F. L.; Cappellano, C. H. Histotechnology. **2015**, 51.
- (27) Zhang, F.; Zhao, J.; Shen, T.; Hidakab, H.; Pelizzetti, E.; Serponed, N. TiO₂-Assisted Photodegradation of Dye Pollutants II. Adsorption and Degradation Kinetics of Eosin in TiO₂ Dispersions under Visible Light Irradiation. 10.
- (28) Cutié, S. S.; Henton, D. E.; Powell, C.; Reim, R. E.; Smith, P. B.; Staples, T. L. The Effects of MEHQ on the Polymerization of Acrylic Acid in the Preparation of Superabsorbent Gels. *Journal of Applied Polymer Science* **1997**, 64 (3), 577–589. [https://doi.org/10.1002/\(SICI\)1097-4628\(19970418\)64:3<577::AID-APP14>3.0.CO;2-V](https://doi.org/10.1002/(SICI)1097-4628(19970418)64:3<577::AID-APP14>3.0.CO;2-V).
- (29) Liang, J.; Liu, F.; Li, M.; Liu, W.; Tong, M. Facile Synthesis of Magnetic Fe₃O₄@BiOI@AgI for Water Decontamination with Visible Light Irradiation: Different Mechanisms for Different Organic Pollutants Degradation and Bacterial Disinfection. *Water Research* **2018**, 137, 120–129. <https://doi.org/10.1016/j.watres.2018.03.027>.
- (30) Meziani, D.; Abdmeziem, K.; Bouacida, S.; Trari, M. Photo-Electrochemical and Physical Characterizations of a New Single Crystal POM-Based Material. Application in Photocatalysis. *Journal of Molecular Structure* **2016**, 1125, 540–545. <https://doi.org/10.1016/j.molstruc.2016.07.006>.